Journal of Hepatocellular Carcinoma

Dovepress
Taylor & Francis Group

Open Access Full Text Article

ORIGINAL RESEARCH

# Comprehensive Evaluation and Validation Reveal Mitochondrial Solute Carrier SLC25A3 as a Novel Prognostic Biomarker and Therapeutic Target in Hepatocellular Carcinoma

Beibei Bie[1], Libing Liu[2], Furong Wang[1], Xianing Meng[1], Mengdi Wu[3], Jin Sun[4]

[1]Department of Pharmacy, Medical School, Xi'an Peihua University, Xi'an, 710125, People's Republic of China; [2]Department of Medical Laboratory Science, Medical School, Xi'an Peihua University, Xi'an, 710125, People's Republic of China; [3]Department of Basic Medical Sciences, Medical School, Xi'an Peihua University, Xi'an, 710125, People's Republic of China; [4]National and Local Joint Engineering Research Center of Biodiagnostics and Biotherapy, The Second Affiliated Hospital of Xi'an Jiaotong University, Xi'an, 710004, People's Republic of China

Correspondence: Beibei Bie, Department of Pharmacy, Medical School, Xi'an Peihua University, Xi'an, 710125, People's Republic of China, Email biepeipei@peihua.edu.cn; Jin Sun, National and Local Joint Engineering Research Center of Biodiagnostics and Biotherapy, The Second Affiliated Hospital of Xi'an Jiaotong University, No. 157 West 5th Road, Xi'an, 710004, People's Republic of China, Email jinsun2014@foxmail.com

Journal of Hepatocellular Carcinoma downloaded from https://www.dovepress.com/
For personal use only.

**Objective:** The Solute carrier family 25 member 3 (SLC25A3), a mitochondrial solute carrier protein, has been implicated in tumor progression. Nonetheless, the connection between SLC25A3 and hepatocellular carcinoma (HCC) remains ambiguous.

**Methods:** The expression, mutation, clinical relevance and immune cell infiltration of SLC25A3 in HCC were investigated via integrated bioinformatics analysis using TCGA data. Hub genes were identified by constructing a protein–protein interaction (PPI) network, and the prognostic risk model was established using univariate Cox and LASSO regression analyses. The potential biological functions of SLC25A3 in HCC were elucidated through GO and KEGG analysis using SLC25A3 co-expressed genes. SLC25A3 expression and promoter methylation status in HCC cells was validated by qRT-PCR and bisulfite sequencing PCR, and the biological function of SLC25A3 in HCC was verified through in vitro loss-of-function experiments.

**Results:** SLC25A3 was significantly upregulated in HCC, accompanied by hypomethylation of its promoter region. Elevated SLC25A3 expression was positively correlated with T stage, histologic grade, AFP level, vascular invasion, residual tumor, and unfavorable prognosis, and served as an independent prognostic factor. SLC25A3 expression was correlated with infiltration of multiple immune cell types. The top 10 SLC25A3 associated-hub genes (SNRPF, SNRPB, SNRPE, SNRPD1, SNRPG, EFTUD2, SNRNP200, SF3A3, SNRPA1, LSM2) were recognized. A four-gene prognostic signature derived from SLC25A3-related hub genes (SNRPB, EFTUD2, SF3A3, and SNRPA1) demonstrated favorable predictive performance. Functional enrichment analysis disclosed that SLC25A3 co-expressed genes were predominantly engaged in RNA splicing, ribosome biogenesis, chromosome segregation, cell cycle and DNA replication. Experimental validation further confirmed that SLC25A3 was remarkably raised in HCC cell lines, with its promoter region displaying a hypomethylated status, and silencing of SLC25A3 suppressed proliferation, migration, and invasion while promoting apoptosis in HCC cells.

**Conclusion:** SLC25A3, a member of the mitochondrial solute carrier family, may function as a novel prognostic biomarker and therapeutic target for HCC.

**Keywords:** hepatocellular carcinoma, SLC25A3, prognosis, proliferation, migration, invasion

## Introduction

Hepatocellular carcinoma (HCC) stands as the chief histological variant of primary liver cancer, holding the sixth position in worldwide cancer occurrence and third in cancer-related deaths.[1,2] The incidence of HCC shows striking geographical variation, with the highest burden in East Asia and sub-Saharan Africa, mainly owing to the widespread occurrence of chronic hepatitis B virus (HBV) and hepatitis C virus (HCV) infections.[3] Additionally, non-viral risk

https://doi.org/10.2147/JHC.S566459
Received: 21 September 2025
Accepted: 16 January 2026
Published: 24 January 2026



© 2026 Bie et al. This work is published and licensed by Dove Medical Press Limited. The full terms of this license are available at https://www.dovepress.com/terms.php and incorporate the Creative Commons Attribution – Non Commercial (unported, v4.0) License (http://creativecommons.org/licenses/by-nc/4.0/). By accessing the work you hereby accept the Terms. Non-commercial uses of the work are permitted without any further permission from Dove Medical Press Limited, provided the work is properly attributed. For permission for commercial use of this work, please see paragraphs 4.2 and 5 of our Terms (https://www.dovepress.com/terms.php).

factors such as alcohol abuse, aflatoxin intake, obesity, diabetes, and non-alcoholic fatty liver disease (NAFLD) have become increasingly important contributors to HCC development.[4,5] Although progress has been made in imaging techniques, surgical interventions, and systemic therapies, HCC continues to be associated with a dismal overall prognosis.[6] Only a limited subset of HCC patients, typically those identified at an early stage, are eligible for potentially curative therapies such as surgery, liver transplantation, or local ablation, while most cases are detected at advanced stages with limited therapeutic options.[7,8] Moreover, the high recurrence and metastasis rates significantly compromise long-term survival. Although molecular targeted therapies and immunotherapies have broadened treatment choices in recent years, their overall efficacy remains modest and drug resistance often emerges.[9,10] Thus, there is a pressing demand for the development of robust biomarkers and novel therapeutic targets that can improve early detection, refine prognostic prediction, and guide more effective treatment strategies for HCC.

The mitochondrial solute carrier family (SLC25) represents the largest subgroup of solute carriers and play pivotal roles in metabolite transport across the mitochondrial membrane, which is crucial for maintaining metabolic homeostasis.[11] Aberrant expression of many SLC25 family members has been implicated in tumorigenesis, tumor advancement, and therapeutic resistance in a variety of cancers,[12] including HCC,[13–16] hinting that SLC25 family genes are considered potential biomarkers or therapeutic targets for cancers. Solute carrier family 25 member 3 (SLC25A3), alternatively known as the mitochondrial phosphate carrier (PiC), is localized to the inner mitochondrial membrane as a transmembrane protein. SLC25A3 primarily mediates phosphate (Pi) transport into the mitochondrial matrix, thus crucially influencing ATP production via oxidative phosphorylation.[17,18] In addition to its classical phosphate transport function, SLC25A3 has also been identified as a mitochondrial copper (Cu) transporter that facilitates the metallation of cytochrome c oxidase (COX),[19] further underscoring its critical role in mitochondrial energy metabolism. A study in osteosarcoma found that SLC25A3 was upregulated in osteosarcoma tissues, and it can act as the target gene of circular RNA circ_0017311 to mediate its promotion of osteosarcoma progression.[20] At present, the connection between SLC25A3 and HCC remains unclear. Interestingly, SLC25A3 expression was markedly reduced in a high-fat diet (HFD)-induced mouse model of NAFLD. Loss of SLC25A3 impaired hepatocellular redox homeostasis by limiting mitochondrial copper accumulation and downregulating key antioxidant genes, including GPX1 and GSR, thereby accelerating NAFLD progression.[21] These observations indicate that SLC25A3 may serve as a pivotal regulator in the pathogenesis of chronic liver disease. However, the potential involvement of SLC25A3 in the occurrence and progression of HCC remains unclear.

To clarify the link between SLC25A3 and HCC, a comprehensive, multi-dimensional analysis of SLC25A3 in HCC were carried out. Specifically, we integrated multi-omics datasets deposited in The Cancer Genome Atlas (TCGA) to systematically illuminate the expression pattern, genetic and epigenetic alterations, clinical associations, immune infiltration, and functional networks of SLC25A3 in HCC. Furthermore, the expression and biological functions of SLC25A3 were validated through in vitro experiments. Collectively, this study seeks to offer fresh perspectives on the clinical value of SLC25A3 in HCC and underscores its potential therapeutic benefits for HCC.

# Material and Methods

## Data Gathering

For the pan-cancer analysis, Toil-reprocessed RNA-seq data covering 29 types of cancers were acquired from the TCGA database via UCSC XENA (https://xenabrowser.net/datapages/). Clinical pathological data of 374 HCC specimens were also accessed from TCGA for analyzing the clinical significance of gene expression. All bioinformatics tasks related to TCGA data were carried out with R language (version 4.2.1). RNA-seq data were filtered and standardized using the "edgeR" package to obtain transcripts per million (TPM) data, which was subsequently log2-transformed for further analysis. Additionally, six normalized expression matrices of GEO datasets (GSE39791, GSE45267, GSE45436, GSE57957, GSE76427, and GSE87630) were retrieved from the GEO database (www.ncbi.nlm.nih.gov/geo/) for confirming the expression trends of SLC25A3 in HCC.

## Bioinformatics Analysis of SLC25A3 Expression and Its Clinical Implication in HCC

Expression profile of SLC25A3 in both pan-cancer and HCC was visualized employing the R package "ggplot2". Associations between SLC25A3 expression and clinical parameters were also explored with the R package "ggplot2". Survival analyses, encompassing overall survival (OS), disease-specific survival (DSS), and progression-free interval (PFI), were executed with R packages "Survival" and "Survminer". To further evaluate prognostic factors influencing OS, univariate and multivariate Cox regression analyses were carried out. A prognostic nomogram, together with a calibration curve, was then established using the R package "rms" and "survival" to estimate 1-, 3-, and 5-year OS probabilities in HCC patients. Moreover, the diagnostic and prognostic predictive capabilities of SLC25A3 was assessed by plotting receiver operating characteristic (ROC) curve with the R package "pROC".

## Genetic Alterations and Methylation Status of SLC25A3 in HCC

The genetic alterations of SLC25A3 in 12 HCC datasets was identified by the cBioPortal (https://www.cbioportal.org), involving the overall genetic alteration situation, the frequency of somatic genetic mutations, the distribution of mutation sites, the impact of genetic alterations on patient prognosis, and the genetic variations of other genes in the genetic alteration samples. The overall methylation level of the SLC25A3 promoter region in HCC was analyzed using UALCAN (https://ualcan.path.uab.edu) and the modification status of individual methylation sites was viewed through MEXPRESS (https://mexpress.ugent.be).

## Analysis of the Relationship Between SLC25A3 and Immune Cell Infiltration

The link between SLC25A3 and immune cell infiltration in HCC was evaluated with the single-sample GSEA (ssGSEA) method using the R package "GSVA" relying on the TCGA data,[22] and the outcomes were subsequently visualized with the R package "ggplot2" in the form of lollipop chart, violin plot and scatter plot, respectively.

## Identification of Co-Expressed Genes of SLC25A3 in HCC

Genes showing positive co-expression with SLC25A3 in HCC were determined by the lights of batch analysis of the correlation between SLC25A3 and 19,448 coding genes, with screening criteria set as |Spearman's r| > 0.4 and adjusted $p$-value < 0.01. The top 10 hub genes were identified through building protein-protein interaction (PPI) network employing STRING (www.stringdb.org), followed by calculations utilizing the CytoHubba plugin of Cytoscape software according to the maximum clique centrality (MCC) method. GO and KEGG enrichment analysis of genes exhibiting positive co-expression with SLC25A3 was carried out employing the R package "clusterProfiler". The involvement of the top 10 hub genes in HCC-related signaling pathways was assessed utilizing the web-based platform GSCALite (http://bioinfo.life.hust.edu.cn/web/GSCALite/).[23]

## Construction of a Prognostic Signature Using Genes Positively Co-Expressed with SLC25A3

The top 10 hub genes were subjected to the least absolute shrinkage and selection operator (LASSO) Cox penalized regression analysis with the R package "glmnet", and genes with non-zero coefficients were subsequently incorporated into a risk score-based prognostic signature. The method for calculating the risk score was as follows:

$$\text{RiskScore} = \sum_{i=1}^{N}(exp \times coef)$$

In the risk score formula, N denotes the number of model genes, exp represents the gene expression level, and coef indicates the corresponding regression coefficient. Using the median value of the risk score as the cutoff, patients with HCC were classified into high- and low-risk categories, and survival differences were examined using Kaplan–Meier analysis. ROC curve was plotted to determine the diagnostic and prognostic accuracy of the model. Cox regression analyses were further applied to examine whether the risk score served as an independent prognostic indicator of OS in

HCC. In addition, based on the risk score, a nomogram combined with calibration curves were developed to forecast 1-, 3-, and 5-year OS probabilities in HCC patients.

## Cell Culture

The immortalized normal human hepatocyte cell line L-O2 along with HCC cell lines (Bel-7404, Hep3B, HepG2, MHCC97H and MHCC97L) were all sourced from the China Center for Type Culture Collection (CCTCC) and preserved in our laboratory. Each cell line was preserved in DMEM with 10% fetal bovine serum (FBS), penicillin at 100 U/mL, and streptomycin at 100 μg/mL, kept at 37°C in a moisture-controlled incubator with 5% $CO_2$.

## Small Interfering RNA (siRNA) Synthesis and Transfection

To silence SLC25A3, three siRNAs specific to SLC25A3 was provided by RiboBio (Guangzhou, China). The specific target sequences are as follows: siRNA-1, 5'-AGUACAAGGGCAUAUUUAA-3'; siRNA-2, 5'-CUCUGGCGCACAUCACUAU -3'; siRNA-3, 5'- GACUCCGUGAAGGUCUACU-3'. A negative control siRNA (5'-UUCUCCGAACGUGUCACGU-3') were also purchased from RiboBio (Guangzhou, China). siRNA transfection was achieved utilizing Lipofectamine™ 3000 Transfection Reagent (ThermoFisher, USA).

## Quantitative Real-Time PCR (qRT-PCR)

Total RNA was isolated from cells with RNAiso Plus (TAKARA, Japan). The synthesis of cDNA for qRT-PCR was achieved employing the Primescript RT reagent kit with gDNA Eraser (TAKARA, Japan), and qRT-PCR assay was carried out with TB Green® Premix Ex Taq™ II (TAKARA, Japan). The relative expression levels of target genes were determined utilizing the $2^{-\Delta\Delta Ct}$ strategy by standardization against β-Actin. All the qRT-PCR primers applied in this investigation are listed as follows: SLC25A3, 5'-CTGGCTCCTATGGAAGCTGCTA-3' and 5'-GTCTCATCCAGAGAGGAGCAAC-3'; β-Actin, 5'-TGGCACCCAGCACAATGAA-3' and 5'-CTAAGTCATAGTCCGCCTAGAAGCA-3'.

## CCK-8 Assay

After seeding $5 \times 10^3$ cells/well into 96-well plates, cells were treated with 10 μL of CCK-8 solution (Dojindo, Japan) and incubated at 37 °C for 90 minutes, after which absorbance was quantified at 450 nm with a microplate reader.

## Colony Formation Test

The cells were planted in a 6-well plate with a concentration of 800 cells per well and cultivated until colonies became apparent. Following this, the cells were stabilized with 4% paraformaldehyde at ambient temperature for 30 minutes, and then were colored with 0.1% crystal violet for 20 minutes. After rinsing and drying, colony formation was recorded via photography and subsequently enumerated.

## Apoptosis Analysis by Flow Cytometry

The cells were collected using trypsin in the absence of EDTA and then dyed with Annexin V-FITC/PI Apoptosis Detection Kit (Yeasen, Shanghai, China). The percentage of apoptotic cells was assessed utilizing the flow cytometry technique.

## Transwell Assays for Cell Migration and Invasion

The capacity of cells to migrate and invade was evaluated using both Matrigel-uncovered and Matrigel-covered 24-well transwell chambers, equipped with transparent PET membranes featuring a pore size of 8.0 μm (Corning, USA). A suspension of $5 \times 10^4$ cells in 200 μL serum-free medium was added to the upper compartment. The lower chamber was filled with culture medium incorporated with 10% FBS to serve as a chemical attractant. Following a 24-hour period for migration detection or a 48-hour period for invasion detection, the cells in the upper chamber were swabbed away, whereas those in the lower chamber were exposed to 4% paraformaldehyde. The cells traversing the PET membrane were stained employing crystal violet and observed through a microscope (100×) to calculate the percentage of staining area.

## Bisulfite Sequencing PCR (BSP)

Genomic DNA was extracted from 5 × $10^6$ cells using the MolPure® Cell/Tissue DNA Kit (Yeasen, Shanghai, China), followed by bisulfite conversion using the Hieff® Superfast DNA Methylation Bisulfite Kit (Yeasen, Shanghai, China). The bisulfite-treated DNA was used as a template for bisulfite sequencing PCR (BSP) to amplify the CpG island region of the SLC25A3 promoter using 2 × EpiArt HS Taq Master Mix (Vazyme, Nanjing, China). BSP primers were designed using MethPrimer software (https://www.methprimer.com/cgi-bin/methprimer/methprimer.cgi). The amplified fragment contained 19 CpG sites, and the primer sequences were as follows: 5′-GTGGAAGGTGAGATTAGATTTTG-3′ and 5′-CCCAATACTTAATTTACTAACCAAAC-3′. The PCR products were purified and cloned into a cloning vector pESI-TA /Blunt (Yeasen, Shanghai, China), followed by transformation into *Escherichia coli* competent cells. Ten independent clones were randomly selected for sequencing, and the methylation status of individual CpG sites was subsequently analyzed.

## Statistical Analysis

All statistical examination were executed with SPSS version 20.0. Student's *t*-test was applied for two-group comparisons, and one-way ANOVA was employed for multiple group analyses. The experimental validation results are presented as mean ± standard deviation (SD) from three biological replicates. A p-value less than 0.05 was set as the benchmark for statistical relevance.

# Results

## SLC25A3 Was Up-Regulated in HCC

To assess the expression trends of SLC25A3 in HCC, transcriptomic data from TCGA were analyzed, including 374 tumor samples, 50 normal tissues, and 50 paired tumor–normal samples. The results uncovered that SLC25A3 expression was dramatically elevated in tumor tissues compared with normal controls in both unpaired and paired cohorts (both $P < 0.001$) (Figure 1A and B). This upregulation was further validated in six independent GEO datasets, in which SLC25A3 levels were consistently elevated in HCC tissues than in adjacent non-tumor tissues (all $P < 0.001$) (Figure 1C–H). Beyond HCC, pan-cancer analysis of TCGA data across 29 tumor types demonstrated aberrant activation of SLC25A3. Specifically, SLC25A3 was markedly upregulated in 17 cancer types, encompassing ACC, CESC, CHOL, DLBC, GBM, KICH, KIRP, LGG, LIHC, PAAD, PRAD, SKCM, STAD, TGCT, THYM, UCEC, and UCS, while downregulation was observed in ESCA, KIRC, LUAD, and LUSC (Figure 1I).

## Genetic Alterations and Methylation Status of SLC25A3 in HCC

To explore genetic alterations status of SLC25A3 in HCC patients, the genetic alterations of SLC25A3 was identified by the cBioPortal (https://www.cbioportal.org) using a total of 3853 samples in 12 HCC datasets (CLCA, Nature 2024; MERiC/Basel, Nat Commun. 2022; MSK, Clin Cancer Res 2018; MSK, Clin Cancer Res 2024; MSK, JCO Precis Oncol 2023; TCGA, GDC; INSERM, Nat Genet 2015; MSK, PLOS One 2018; AMC, Hepatology 2014; RIKEN, Nat Genet 2012; TCGA, Firehose Legacy; TCGA, PanCancer Atlas). As demonstrated in Figure 2A and B, the overall mutation frequency of SLC25A3 in HCC is approximately 0.3%, mainly involving missense mutations and gene amplification. Kaplan–Meier survival analyses revealed that genetic alterations in SLC25A3 were not significantly associated with overall survival (OS, $P = 0.204$) or disease-free survival (DFS, $P = 0.089$) (Figure 2C). As shown in Figure 2D, the somatic mutation frequency of SLC25A3 in HCC is approximately 0.1% and the mutation sites are mainly located in the mitochondrial carrier (Mito_carr) domain of the SLC25A3 protein. We also found that the alteration frequency of the NAV3, TP53, LGR5, ULK1, UTP20, MEP1A, EP400 and LRRIQ1 genes in the SLC25A3 mutant samples were remarkably elevated compared to those in the group without mutations (Figure 2E). Furthermore, we observed a marked decrease in DNA methylation within the promoter region of SLC25A3 in HCC tissues against benign counterparts (Figure 2F), and several DNA methylation sites whose methylation levels were significantly negatively correlated with the expression levels of SLC25A3 were identified, including cg16871561, cg00763151, cg02923274, cg12074252, cg09526886, cg20303850 and cg16711096 (Figure 2G).

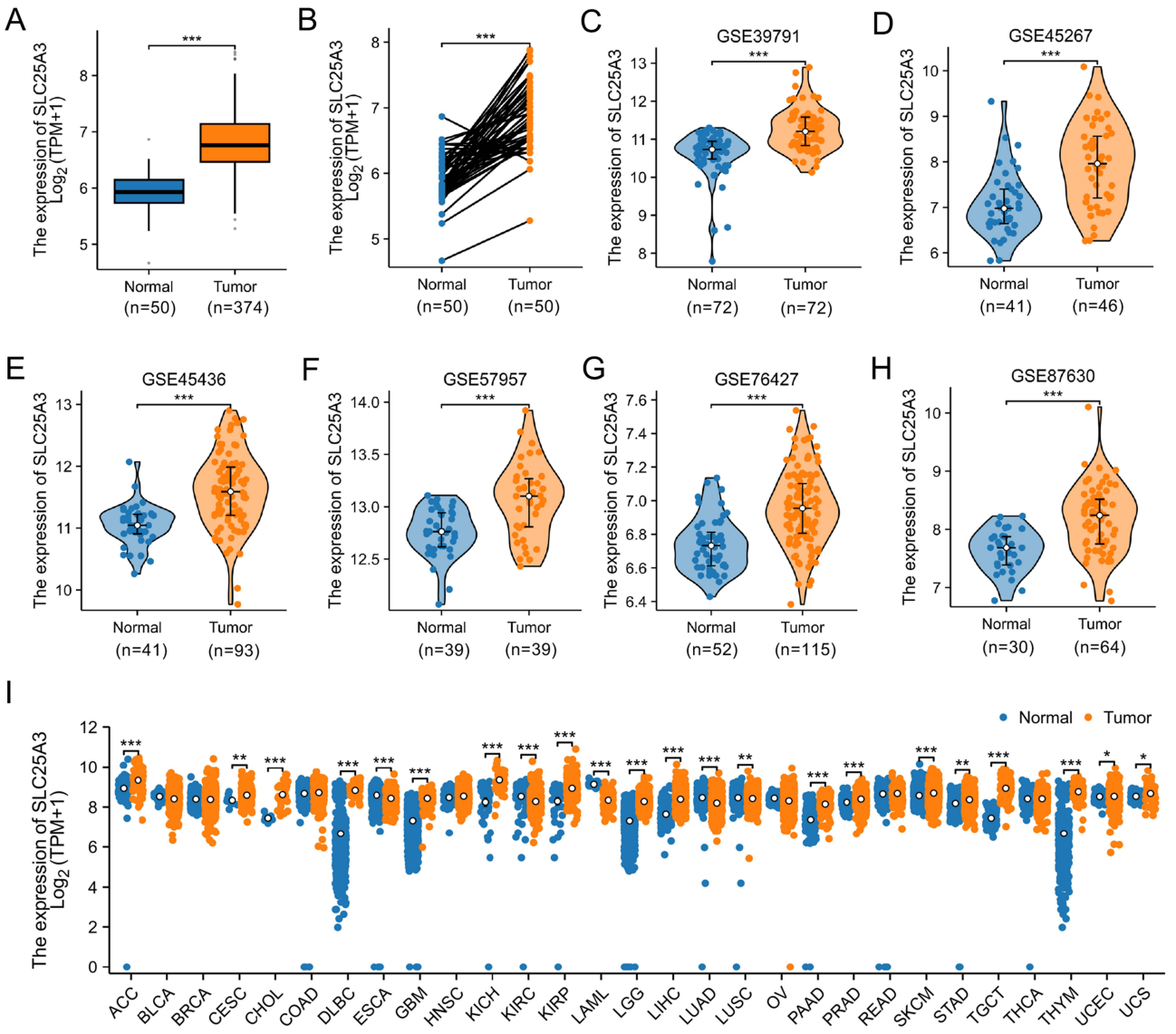


**Figure 1** SLC25A3 was up-regulated in HCC. SLC25A3 expression in unpaired (**A**) and paired (**B**) HCC tissues were analyzed using TCGA data and validated in six GEO datasets (**C–H**). (**I**) Pan-cancer analysis of SLC25A3 expression across 29 cancer types based on TCGA data. *$P < 0.05$, ** $P < 0.01$, *** $P < 0.001$.

**Abbreviations**: ACC, adrenocortical carcinoma; BLCA, bladder urothelial carcinoma; BRCA, breast invasive carcinoma; CESC, cervical squamous cell carcinoma; CHOL, cholangiocarcinoma; COAD, colon adenocarcinoma; DLBC, diffuse large B-cell lymphoma; ESCA, esophageal carcinoma; GBM, glioblastoma multiforme; HNSC, head and neck squamous cell carcinoma; KICH, kidney chromophobe; KIRC, kidney renal clear cell carcinoma; KIRP, kidney renal papillary cell carcinoma; LAML, acute myeloid leukemia; LGG, brain lower grade glioma; LIHC, liver hepatocellular carcinoma; LUAD, lung adenocarcinoma; LUSC, lung squamous cell carcinoma; OV, ovarian serous cystadenocarcinoma; PAAD, pancreatic adenocarcinoma; PRAD, prostate adenocarcinoma; READ, rectum adenocarcinoma; SKCM, skin cutaneous melanoma; STAD, stomach adenocarcinoma; TGCT, testicular germ cell tumors; THCA, thyroid carcinoma; THYM, thymoma; UCEC, uterine corpus endometrial carcinoma; UCS, uterine carcinosarcoma.

## Association Between SLC25A3 Expression and Clinical Traits of HCC Patients

As illustrated in Figure 3A–E, elevated SLC25A3 expression in HCC tissues showed significant positive associations with T stage, histological grade, AFP levels, vascular invasion, and residual tumor status (all $P < 0.05$). Kaplan–Meier survival curves (Figure 3F–H) further demonstrated that patients with high SLC25A3 expression had markedly worse OS and DSS compared with those exhibiting low expression (both $P < 0.05$), whereas no significant association was observed with PFI, implying that elevated SLC25A3 could serve as a predictor of unfavorable outcomes in HCC. Univariate Cox regression study uncovered that SLC25A3 expression (HR = 1.715, $P = 0.002$), T stage (HR = 2.598, $P < 0.001$) and M stage (HR = 4.077, $P = 0.017$) showed a notable link with OS (Figure 3I). Subsequent multivariate Cox regression confirmed that SLC25A3 expression (HR = 1.834, $P = 0.008$) represents an independent prognostic element for OS in HCC (Figure 3J).

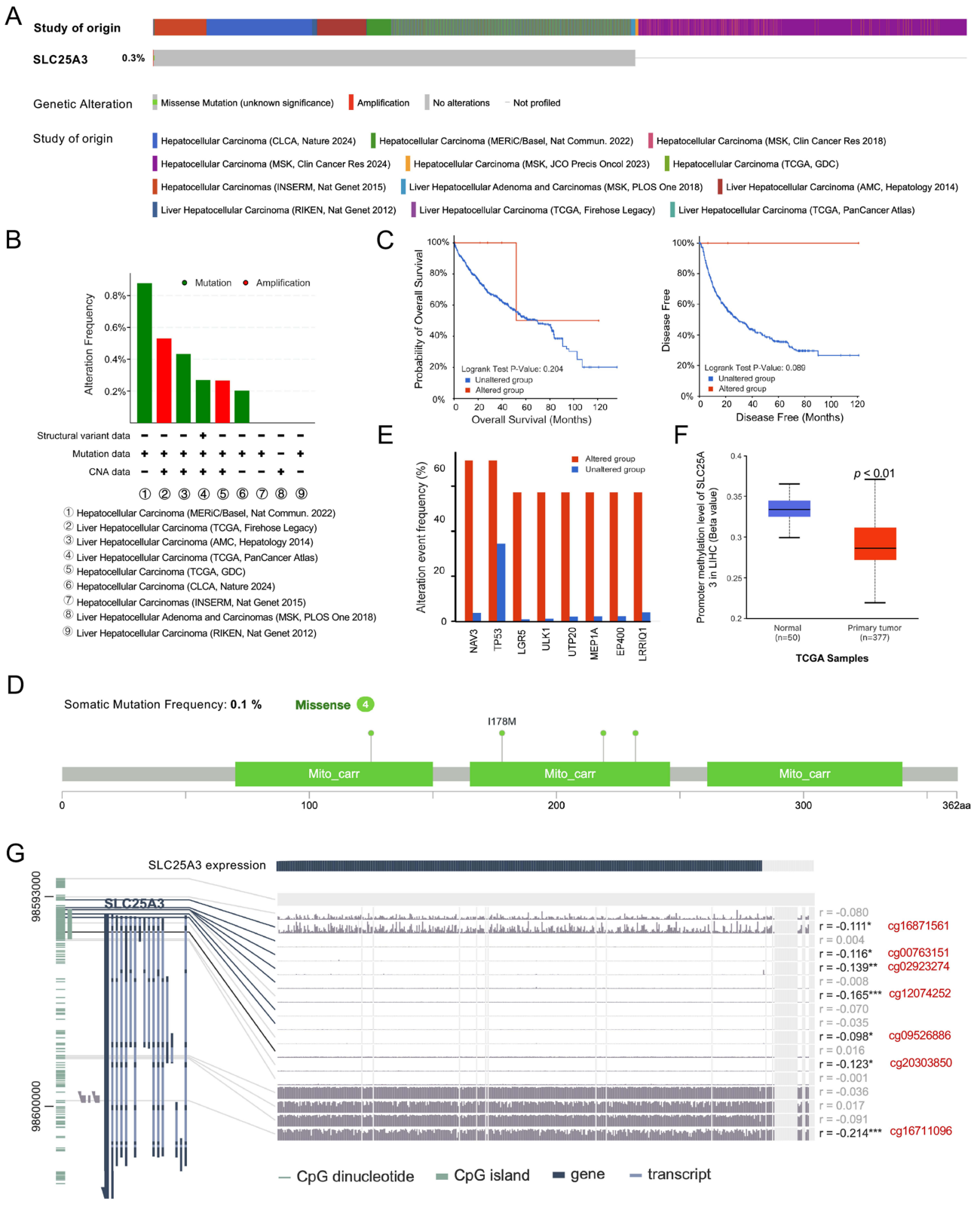


**Figure 2** Genetic alterations and methylation status of SLC25A3 in HCC. (**A**) Overall genetic alterations of SLC25A3 in 12 HCC datasets. (**B**) Summary of SLC25A3 genetic alteration in 9 HCC datasets. (**C**) Kaplan-Meier plots of OS and DFS in patients with or without genetic alteration of SLC25A3 in HCC. (**D**) Distribution of SLC25A3 mutation sites. (**E**) Genes with high-frequency genetic variations in the SLC25A3 mutation cohort. (**F**) Overall DNA methylation level of the SLC25A3 promoter revealed by UALCAN. (**G**) The methylation modification status of single site within SLC25A3 region in HCC revealed by MEXPRESS. *$P$ < 0.05, ** $P$ <0.01, *** $P$ <0.001.


https://doi.org/10.2147/JHC.S566459

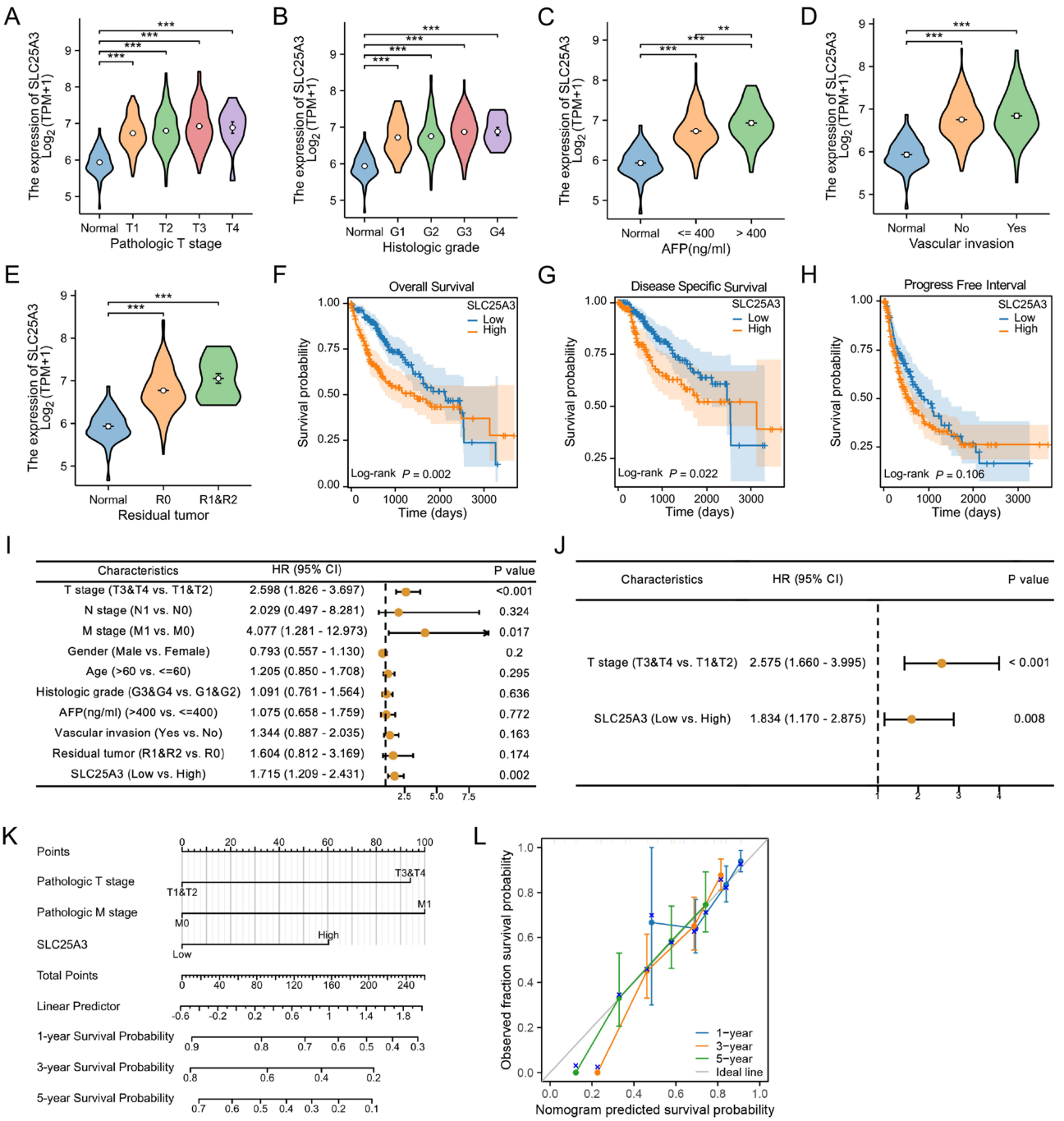


**Figure 3** Association between SLC25A3 expression and clinical characteristics of HCC patients. Violin plot displaying the association between SLC25A3 expression and T stage (**A**), histological grade (**B**), AFP level (**C**), vascular invasion (D), residual tumor (**E**). Kaplan-Meier survival curves demonstrating relationship of SLC25A3 expression with overall survival (**F**), disease specific survival (**G**) and progress free interval (**H**). Forest plot showing results of univariate (**I**) and multivariate (**J**) Cox regression analysis of SLC25A3 level for overall survival. (**K**) The nomogram model predicting 1-, 3- and 5-year overall survival. (**L**) Calibration curves of the nomogram prediction model. *** *P* <0.01, *** *P* <0.001.

Furthermore, a nomogram integrating SLC25A3 expression and other key prognostic elements from univariate analysis was developed to forecast 1-, 3-, and 5-year OS (Figure 3K). The calibration plots disclosed a remarkable agreement between forecasted and actual survival outcomes, highlighting the robustness and reliability of the model (Figure 3L).

## Assessment of the Diagnostic and Prognostic Significance of SLC25A3 in HCC

To determine the diagnostic utility of SLC25A3 in HCC, ROC curve analyses were performed. As illustrated in Figure 4A–D, SLC25A3 expression displayed strong diagnostic performance for distinguishing HCC (AUC = 0.925), T1&T2 stage tumors (AUC = 0.920), histological grades G1&G2 (AUC = 0.915), and residual tumor status (AUC = 0.921). In addition, time-dependent ROC study demonstrated that SLC25A3 expression exhibited moderate predictive capacity for OS at 1-, 3-, and 5-year intervals (AUC = 0.687, 0.608, and 0.606, respectively) and for DSS (AUC = 0.667, 0.586, and 0.591, respectively) (Figure 4E and F).

## The Link Between SLC25A3 Expression and Immune Cell Infiltration in HCC

Previous studies have reported that SLC25 family genes, including SLC25A19 and SLC25A35, are closely associated with immune cell infiltration in HCC.[13,24] To investigate the specific connection between SLC25A3 and the penetration of immune cell in HCC, we examined the link between SLC25A3 expression and immune cell infiltration across 20 immune cell subtypes in HCC tissues (Figure 5A). SLC25A3 expression was discovered to have an inverse relationship with Th17 cells, $CD8^+$ T cells, B cells, plasmacytoid dendritic cells (pDCs), eosinophils, and neutrophils (|Spearman's r| > 0.1, $P < 0.05$), whereas positive correlations were observed with Th2 cells, follicular helper T (TFH) cells, and macrophages (Figure 5B and C).

## Co-Expression Network Analysis of SLC25A3 in HCC

To characterize the co-expression landscape of SLC25A3 in HCC, genes positively correlated with SLC25A3 expression were systematically screened. A total of 1,044 genes exhibiting strong positive correlations were identified based on the criteria of |Spearman's r| > 0.4 and adjusted $P < 0.01$ (Supplementary Table 1). A PPI network constructed from these co-expressed genes revealed 10 hub genes (SNRPF, SNRPB, SNRPE, SNRPD1, SNRPG, EFTUD2, SNRNP200, SF3A3, SNRPA1, LSM2), whose expression levels were robustly positively correlated with SLC25A3 in HCC (Figure 6A–C). Moreover, all 10 hub genes were significantly upregulated in HCC tissues (Figure 6D) and were positively associated with advanced pathologic T stage, higher histological grade, and poorer overall survival (OS) (all $P < 0.05$) (Figure 7A–C).

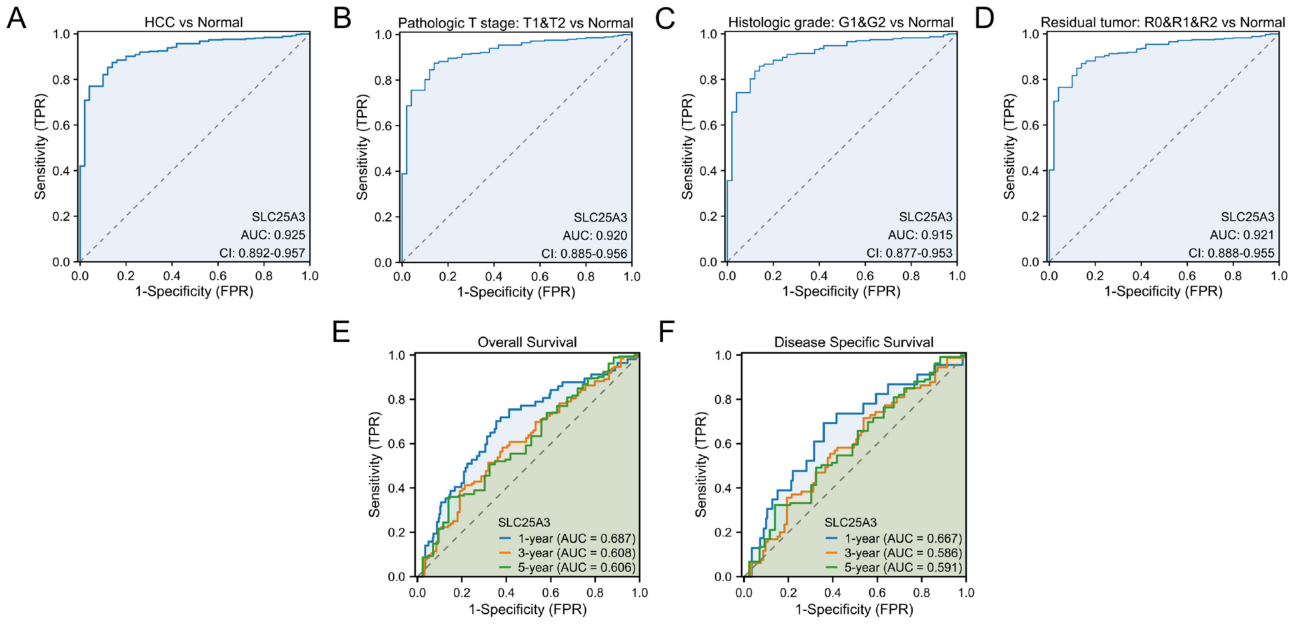


**Figure 4** Diagnostic and prognostic ROC curves of SLC25A3 level in HCC. (**A**) HCC vs normal. (**B**) T stage T1&T2 vs normal. (**C**) histologic grade G1&G2 vs normal. (**D**) Residual tumor R0&R1&R2 vs normal. (**E**) 1-, 3-, and 5-year overall survival. (**F**) 1-, 3-, and 5-year disease specific survival.


https://doi.org/10.2147/JHC.S566459

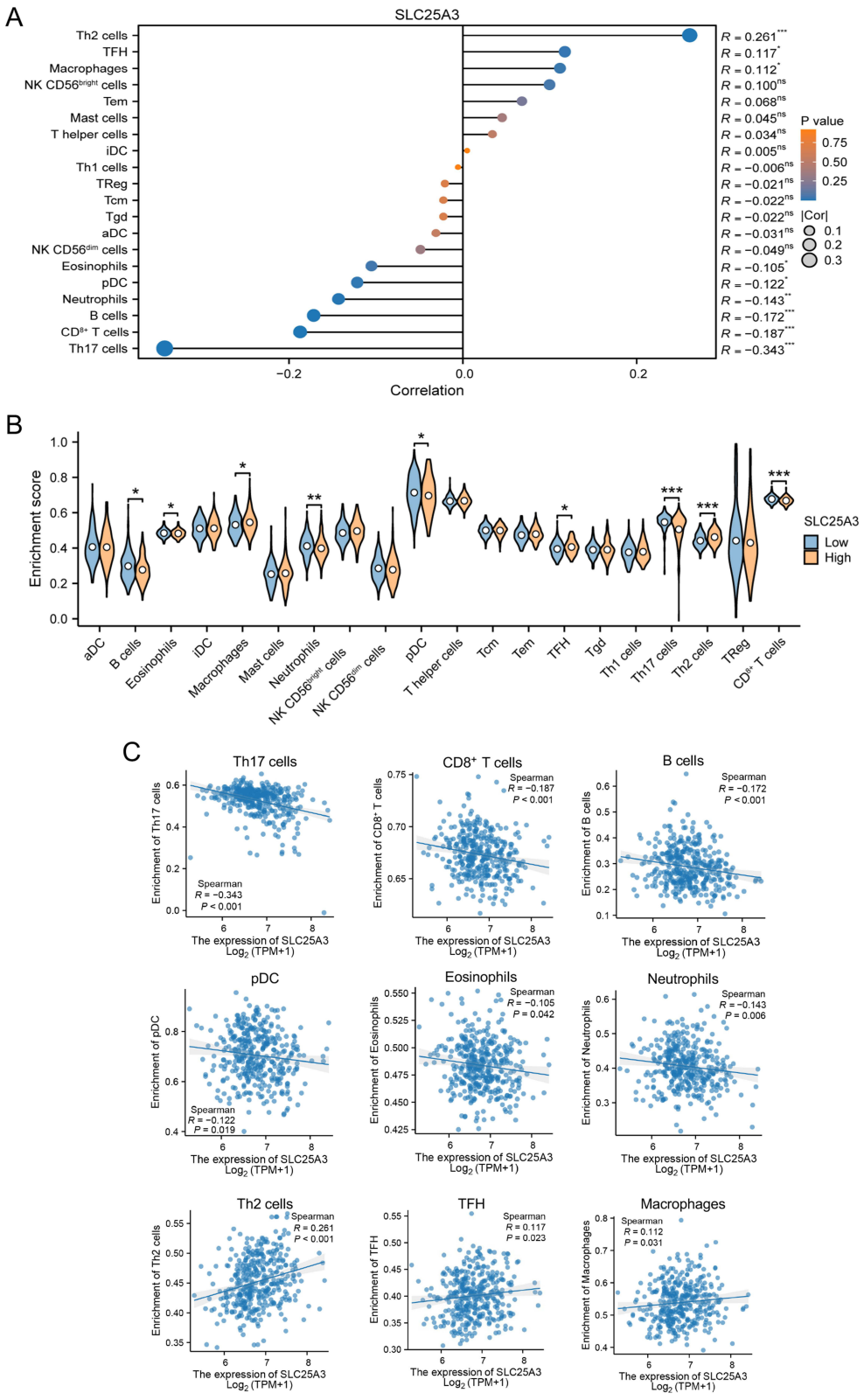


**Figure 5** Relevance between SLC25A3 level and immune cell infiltration in HCC. (**A**) Lollipop chart showing the correlation between SLC25A3 level and 20 different types of immune cells. (**B**) Violin plot displaying the infiltration degree of 20 immune cell types in HCC patients with high and low expression of SLC25A3. (**C**) The scatter plot showing the correlation between the expression level of SLC25A3 and the degree of immune cell enrichment in HCC. NS represents not significant, *$P < 0.05$, **$P < 0.01$, ***$P < 0.001$.

**Abbreviations**: aDC, activated dendritic cells; iDC, immature dendritic cells; pDC, plasmacytoid dendritic cells; NK, natural killer cells; Tcm, T central memory; Tem, T effector memory; TFH, T follicular helper cells; Tgd, gamma delta T cells; Th, T helper cells; Treg, regulatory T cells.

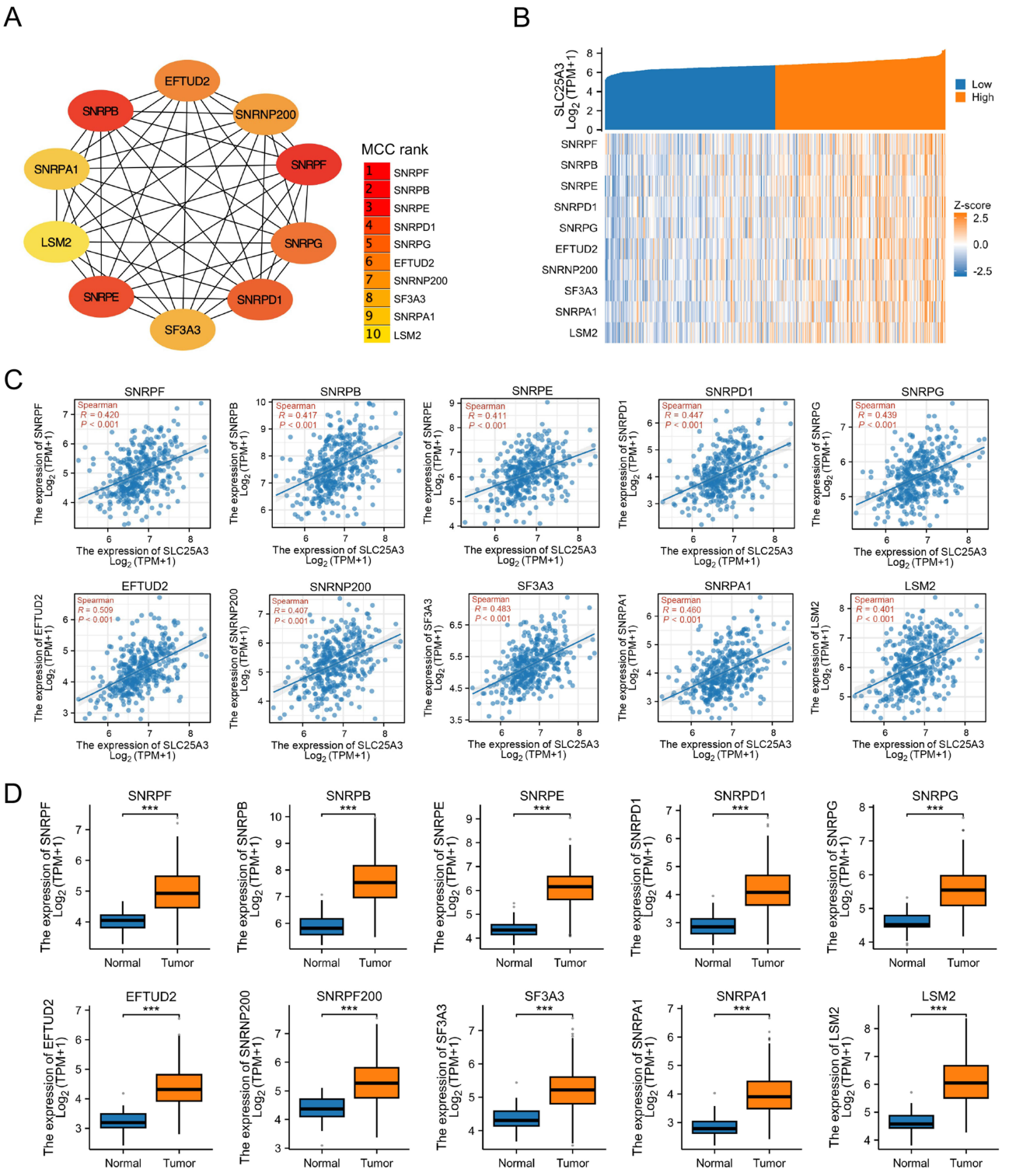


**Figure 6** Construction of protein-protein interaction network based on positively co-expressed genes of SLC25A3 in HCC. (**A**) The top 10 hub genes were identified based on the MCC methods. The correlation between the expression of hub genes and SLC25A3 in HCC was shown by heatmap (**B**) and scatter plot (**C**). (**D**) Analysis of the expression status of the top 10 hub genes in HCC based on TCGA data. ***$P < 0.001$.

## Establishment and Evaluation of a Hub-Gene-Based Prognostic Model from SLC25A3 Co-Expressed Genes in HCC

Following LASSO regression analysis, a prognostic signature was established based on four hub genes (SF3A3, EFTUD2, SNRPB, SNRPA1) (Figure 8A and B), and individual risk scores were determined employing the formula:


https://doi.org/10.2147/JHC.S566459

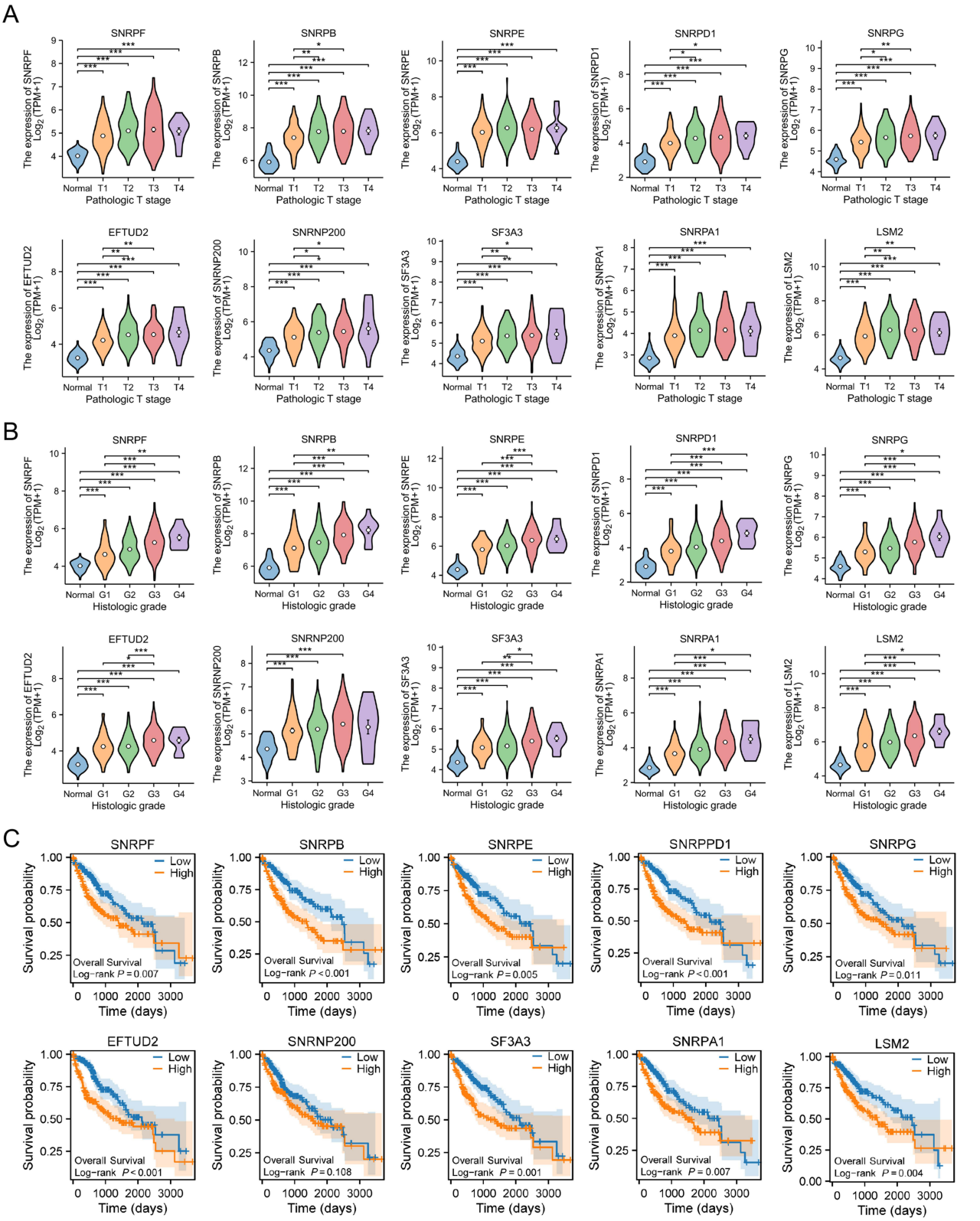


**Figure 7** The clinical significance of the top 10 hub genes in HCC. (**A**) T stage. (**B**) Histologic grade. (**C**) Overall survival. *$P$ < 0.05, ** $P$ <0.01, *** $P$ <0.001.

Risk score = (SF3A3 × 0.502) + (EFTUD2 × 0.098) + (SNRPB × 0.129) + (SNRPA1 × 0.003). To examine the prognostic utility of this model, patients were allocated to high- and low-risk cohorts using the median risk score as a cutoff. As shown in Figure 8C, individuals classified as high-risk experienced elevated mortality and decreased survival times, which was further confirmed by Kaplan–Meier analysis demonstrating significantly worse OS for the high-risk group ($P < 0.01$) (Figure 8D). Time-dependent ROC analysis signified satisfactory predictive accuracy of the model for 1-, 3-, and 5-year OS, with all AUC values exceeding 0.6 (Figure 8E). Investigations employing both univariate and multivariate Cox regression uncovered a notable correlation between the risk score and OS, serving as an independent predictive factor (HR = 1.648, $P = 0.005$) (Figure 8F and G). Furthermore, a nomogram incorporating the risk score along with clinical variables consisting of age, gender, T, N, M stages, and histological grade was constructed, highlighting the risk score as a key determinant among these parameters (Figure 8H). Calibration plots confirmed the model's robust predictive capability for 1-, 3-, and 5-year OS probabilities (Figure 8I).

## Prediction of Potential Roles and Mechanisms of SLC25A3 in HCC Based on Co-Expression Networks

To explore potential biological functions and pathways of SLC25A3 in HCC, GO and KEGG enrichment analyses were performed based on SLC25A3 co-expressed genes. The top 10 enriched terms in biological processes (BP), cellular components (CC), molecular functions (MF), and KEGG routeways was identified. The results uncovered that these genes were predominantly associated with RNA splicing, ribosome biogenesis, chromosome segregation, cell cycle regulation, and DNA replication (Figure 9A–D). Furthermore, the GSCALite study indicated a primary link between the top 10 hub genes and activation of the cell cycle and epithelial–mesenchymal transition (EMT) in HCC (Figure 9E).

## Experimental Verification of SLC25A3 Expression and Its Functional Roles in HCC

For elucidating the status of SLC25A3 expression in HCC, we detected the expression of SLC25A3 in five HCC cell lines (Bel-7404, Hep3B, HepG2, MHCC97H and MHCC97L) and human normal hepatocyte cell line L-O2. As exhibited in Figure 10A, there was a notable increase in the expression of SLC25A3 across all HCC cell lines that were detected, aligning with the previously mentioned bioinformatics discoveries.

To investigate the biological roles of SLC25A3 in HCC, MHCC97L and HepG2 cell lines, which exhibit high SLC25A3 expression, were selected for loss-of-function experiments (Figure 10A). Three siRNAs were designed to mute the expression of SLC25A3 in HCC cells, and all of them displayed effective knockdown effects (Figure 10B). Subsequently, we selected the two siRNAs (siRNA-1 and siRNA-2) with the most effective knockdown effect for functional studies. The impact of SLC25A3 knockdown on HCC cell proliferation, apoptosis, migration, and invasion was assessed following siRNA transfection. As demonstrated in Figure 10C–G, silencing SLC25A3 markedly reduced cell growth, colony establishment, migration, and invasion, while markedly increasing the proportion of apoptotic cells. In addition, the methylation status of the CpG island within the SLC25A3 promoter region in MHCC97L and HepG2 cell lines was validated using bisulfite sequencing PCR, and the results indicated that the CpG island in the SLC25A3 promoter exhibits an extremely low level of DNA methylation in both HCC cell lines (Figure 10H and I), which is consistent with the findings derived from bioinformatics database analyses. Collectively, these discoveries propose that SLC25A3 functions as a promoter of malignant phenotypes in HCC.

# Discussion

SLC25 family genes have recently attracted considerable attention in HCC research. As the principal channels for metabolite exchange across the inner mitochondrial membrane, SLC25 proteins directly govern cellular energy metabolism, redox homeostasis and apoptotic signaling; dysregulation of these carriers is closely associated with HCC initiation and progression.[14,15] Multiple SLC25 paralogs are aberrantly expressed in HCC, where they contribute to metabolic reprogramming that supports tumor proliferation, survival and drug resistance.[13,25] Beyond metabolic roles, several SLC25 members have been linked to prognosis and to remodeling of the tumor immune microenvironment, suggesting their value as biomarkers and potential therapeutic targets.[12,24,26] Therefore, the exploration of novel SLC25 family genes

 https://doi.org/10.2147/JHC.S566459 

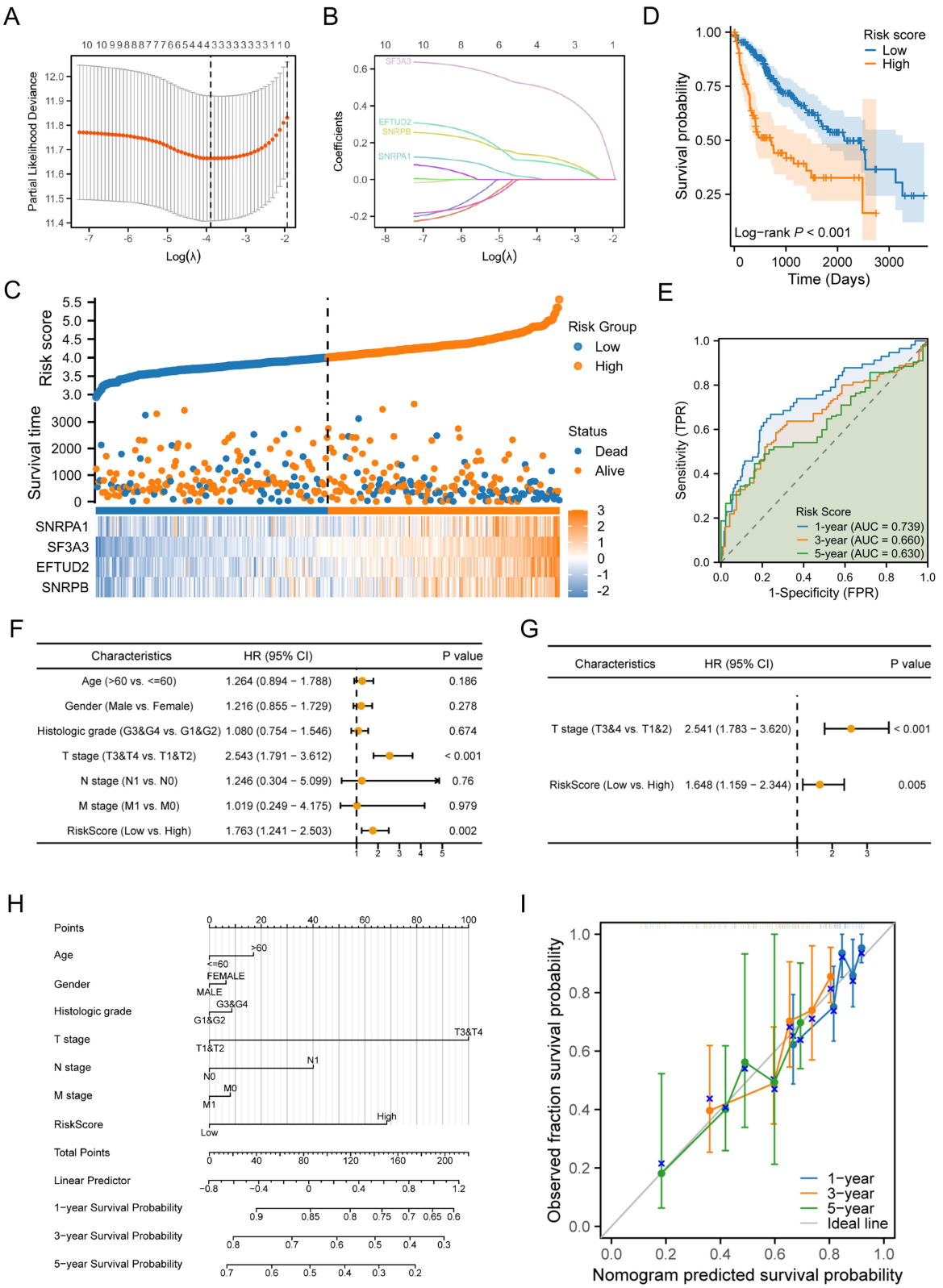


**Figure 8** Construction of the HCC prognostic risk model based on 4 hub genes. (**A**) Cross-validation to select the optimal tuning parameter (λ). (**B**) LASSO coefficient profiles of the 10 hub genes. (**C**) The risk score, survival status, and expression heatmap of 4 hub genes in patients with HCC. (**D**) Kaplan Meier curves showing the overall survival of HCC patients in the high-risk and low-risk groups. (**E**) The predictive efficiency of the risk score for 1-, 3-, 5-year overall survival was verified by the ROC curve. Forest plot showing results of univariate (**F**) and multivariate (**G**) Cox regression analysis of the risk score for overall survival. (**H**) The Nomogram for predicting the 1-, 3-, and 5-year overall survival using the risk scores and clinical features in HCC. (**I**) Calibration plots for assessing the predictive performance of the nomogram.

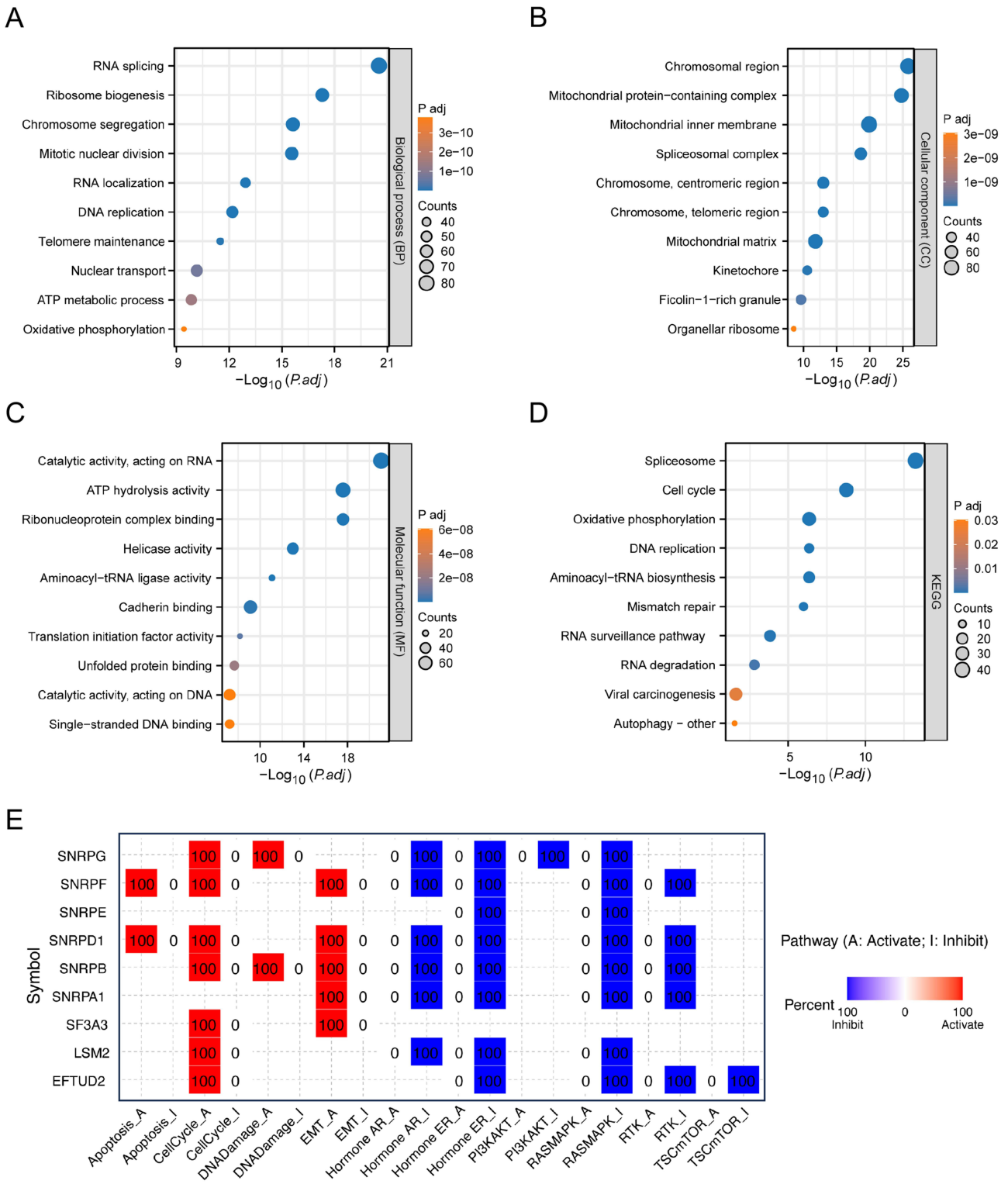


**Figure 9** Functional enrichment analysis of genes significantly positively co-expressed with SLC25A3 in HCC. Bubble plot showing the top 10 enriched terms for biological process (**A**), cellular component (**B**), Molecular function (**C**) as well as KEGG (**D**). (**E**) The association of the top 10 hub genes with some tumour-related signaling pathways in pan-cancer was analyzed by GSCALite.

related to HCC will be beneficial for providing effective diagnostic indicators and therapeutic targets for HCC. In this study, we performed a comprehensive evaluation of SLC25A3 in HCC by integrating bioinformatics analysis with experimental validation, aiming to elucidate its clinical significance and biological functions.


https://doi.org/10.2147/JHC.S566459

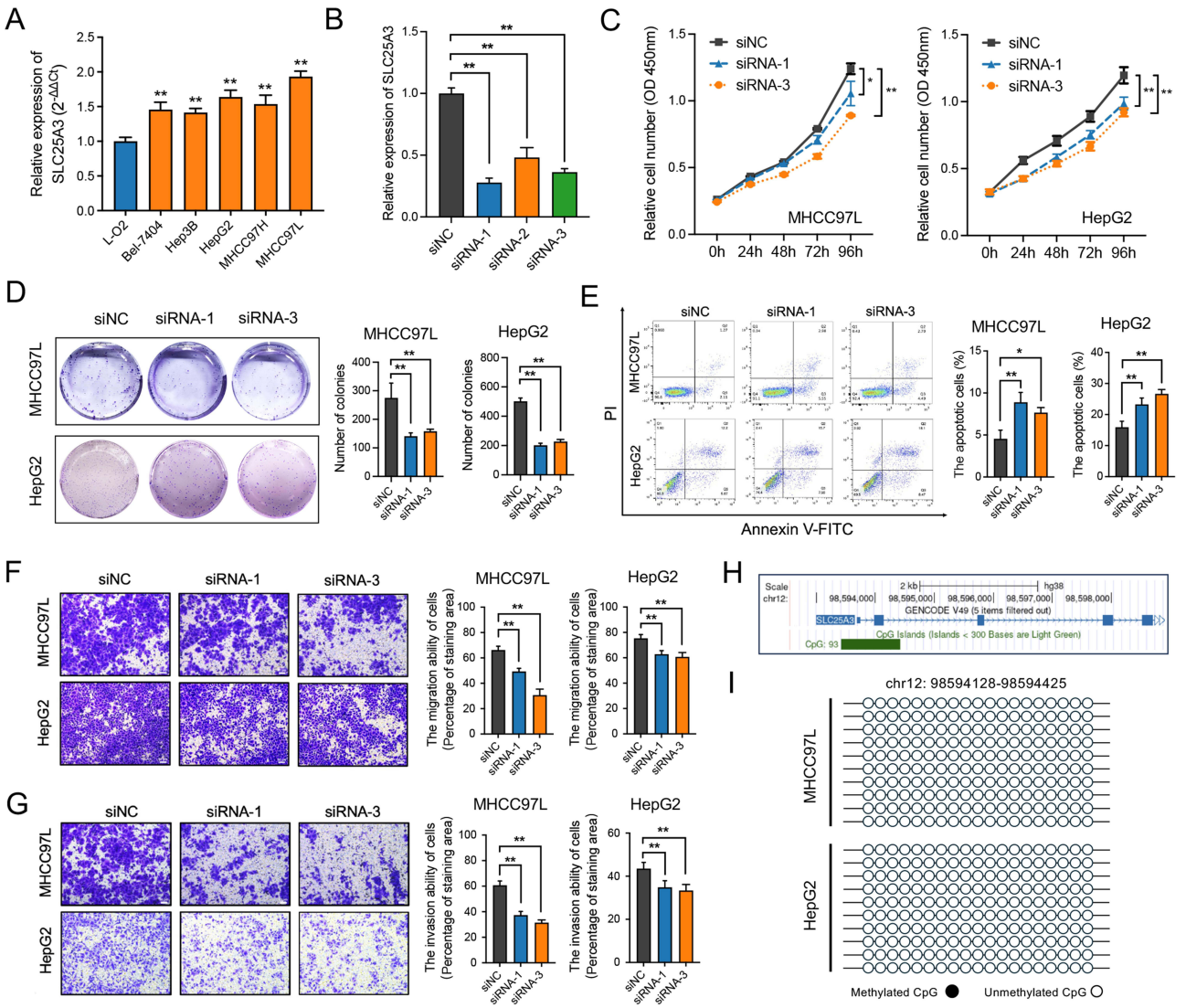


**Figure 10** Experimental validation of the expression of SLC25A3 and its biological roles in HCC. (**A**) Validation of the expression status of SLC25A3 in HCC cell lines by qRT-PCR. (**B**) The knockdown efficiency of siRNAs targeting SLC25A3 in HCC cells was evaluated by qRT-PCR. The proliferative ability of HCC cells was detected by CCK8 (**C**) and colony formation assay (**D**). (**E**) The cell apoptosis was determined by flow cytometry. The migration (**F**) and invasion (**G**) of HCC cells was assessed by transwell assay, scale bar = 50 μm. (**H**) The CpG island near the promoter of SLC25A3 was shown by UCSC Genome Browser. (**I**) The hypomethylation of the SLC25A3 promoter in HCC cell lines was validation by bisulfite sequencing PCR. *$P < 0.05$, **$P < 0.01$.

First, SLC25A3 was revealed to show a notable increase in expression in HCC when contrasted with benign liver tissues, a finding consistently validated across TCGA and multiple GEO cohorts. The findings of the Pan-Cancer evaluation indicate that SLC25A3 was elevated in most cancer types, including HCC, suggesting that SLC25A3 may have a carcinogenic effect and was a potential tumor diagnostic marker. Furthermore, we found the mutation frequency of SLC25A3 in HCC was relatively low and its expression was partly regulated by DNA methylation, indicating that epigenetic mechanisms rather than genetic alterations may underlie its dysregulation. Moreover, the observed co-alteration of genes such as TP53 and NAV3 in SLC25A3-mutant cases implies potential cooperative oncogenic interactions.

Secondly, high SLC25A3 expression in HCC was uncovered to be closely linked with progressive clinicopathological traits, encompassing higher T stage, histological grade, AFP levels, vascular invasion, and residual tumor. Moreover, survival analyses and Cox regression models implied that SLC25A3 serves as an independent prognostic predictor of risk, further supporting its potential as a clinically relevant biomarker. The diagnostic accuracy of SLC25A3 was also robust, as reflected by high AUC values in ROC analyses across multiple subgroups, indicating that SLC25A3 holds

promise as an innovative molecular indicator for the early detection and prediction of HCC. Moreover, we disclosed that SLC25A3 expression correlated with altered immune cell infiltration, characterized by decreased Th17, $CD8^+$ T cells, B cells, pDC, eosinophils and neutrophils but increased Th2, TFH, macrophage populations, implying a role in shaping an immunosuppressive tumor microenvironment. Recently, several other members of the SLC25 family have also been reported to be associated with immune cell infiltration in HCC. For example, SLC25A35 was found to be positively correlated with the infiltration of B cells, $CD8^+$ T cells, $CD4^+$ T cells, macrophages, neutrophils, and DC.[13] In contrast, SLC25A19 was reported to be negatively correlated with DC, Th17 cells, neutrophils, pDC, mast cells, and B cells, while showing a positive correlation with Th2 cells.[24] Collectively, these findings highlight SLC25A3 not only as a prognostic and diagnostic biomarker but also as a possible immunometabolic regulator in HCC.

Thirdly, the importance in biology of SLC25A3 in HCC was highlighted through constructing co-expression network and conducting functional enrichment. The co-expressed genes of SLC25A3 were primarily enriched in routeways linked to RNA splicing, ribosome biogenesis, and cell cycle regulation, suggesting that SLC25A3 may exert oncogenic functions by bridging mitochondrial metabolism with transcriptional and post-transcriptional regulation. Notably, aberrant RNA splicing is increasingly recognized as a major driver of HCC advancement and therapeutic resistance.[27,28] Furthermore, a predictive model consisting of four hub genes (SNRPB, EFTUD2, SF3A3, and SNRPA1) derived from the top 10 SLC25A3 co-expressed hub genes was established using LASSO regression, and this model exhibited robust predictive performance and was recognized as an independent predictive element for HCC. Notably, each of the four hub genes have been reported to be critical contributors to HCC progression. For instance, a recent finding demonstrated that SNRPB can promote the HCC development by regulating the alternative splicing of EZH2.[29] Collectively, these findings underscore the potential clinical utility of incorporating SLC25A3-related molecular features into risk stratification systems for HCC.

In the end, we experimentally validated the oncogenic role of SLC25A3 in HCC. Consistent with the bioinformatics analysis, SLC25A3 expression was markedly elevated in HCC cell lines compared with normal hepatocytes, confirming its abnormal activation at the cellular level. Functional assays further demonstrated that silencing SLC25A3 markedly impaired proliferation, colony formation, migration, and invasion, and concurrently triggered apoptotic cell death, indicating that SLC25A3 contributes to multiple malignant phenotypes of HCC and may represent a promising target for therapeutic intervention in HCC. Notably, most SLC25 family genes that have been functionally characterized in HCC are acting as oncogenes. For instance, SLC25A35 was recently discovered to promote fatty acid oxidation and mitochondrial biogenesis through elevating PGC-1α, thereby accelerating the HCC progression.[13] SLC25A19 was found to be able to promote the progression of HCC by inhibiting ferroptosis.[24] Interestingly, SLC25A20 was found to be markedly reduced in HCC, and acts as a negative regulator of tumor progression by facilitating fatty acid oxidation, thereby restraining cancer growth and metastatic potential.[15]

Despite the present study providing preliminary evidence for the involvement of SLC25A3 in HCC, several limitations should be acknowledged. First, the bulk of our analyses relied on retrospective public datasets, including TCGA and GEO, which are inherently susceptible to selection bias, and prospective validation in larger, well-characterized clinical cohorts is still warranted. Second, the association between SLC25A3 expression and immune cell infiltration was mainly derived from computational deconvolution and therefore reflects correlative rather than causal relationships. Functional immune-related experiments, such as immune cell co-culture assays or in vivo modeling, were not performed in the current study, and the mechanisms by which SLC25A3 may modulate the tumor immune microenvironment in HCC require further experimental validation. Third, the oncogenic role of SLC25A3 in HCC was evaluated mainly through in vitro cellular experiments, and future studies should employ animal models to further elucidate the pro-tumorigenic function and underlying mechanisms of SLC25A3 in vivo.

## Conclusion

The present study comprehensively disclosed that SLC25A3 is markedly upregulated in HCC and functions as an oncogenic molecule, serving as a prognostic and diagnostic biomarker while also representing a promising therapeutic target. These findings provide a theoretical foundation for future mechanistic exploration and clinical translational research on SLC25A3 in HCC.

## Data Sharing Statement

The data that support the findings of this study are available from the corresponding author upon reasonable request.

## Ethics Statement

Tumor tissue gene expression profiles and clinical information data involved in this study were sourced from the publicly available TCGA database, which adheres to the NIH Genomic Data Sharing Policy with fully de-identified datasets containing no directly or indirectly identifiable private information. This study complies with the TCGA Data Use Certification Agreement (DUCA) for non-commercial research purposes. Secondary analysis of public data aligns with the ethical principles of the Declaration of Helsinki. The Ethics Committee of Xi'an Peihua University approved the study and waived the requirement for informed consent (XPHU2025008).

## Acknowledgments

We would like to thank the other members of our research team for their assistance. We are also grateful to the TCGA and GEO database for providing access to the public data.

## Author Contributions

All authors made a significant contribution to the work reported, whether in conception, study design, execution, data acquisition, analysis, interpretation, or all these areas; took part in drafting, revising, or critically reviewing the article; gave final approval of the version to be published; agreed on the journal for submission; and agree to be accountable for all aspects of the work.

## Funding

This research was funded by Research Project of Xi'an Peihua University (PHKT2304), Natural Science Foundation Research Program of Shaanxi Province of China (2023-JC-YB-750 and 2023-JC-YB-700), Scientific Research Program of Education Department of Shaanxi Province (20JK0821), the Youth Innovation Team of Shaanxi Universities (Research on Brain Injury and Repair Research Team) and Scientific Research Project of Youth Innovation Team of Shaanxi Universities (No. 24JP137), and the Key Laboratory of Shaanxi Universities (Brain Injury and Drug Prevention Research Laboratory) and Scientific Research Project of Key Laboratory of Shaanxi Universities (No. 24JS038).

## Disclosure

The authors declare no conflicts of interest in this work.

## References

1. Siegel RL, Giaquinto AN, Jemal A. Cancer statistics, 2024. *CA Cancer J Clin*. 2024;74(1):12–49. doi:10.3322/caac.21820
2. Bray F, Laversanne M, Sung H, et al. Global cancer statistics 2022: GLOBOCAN estimates of incidence and mortality worldwide for 36 cancers in 185 countries. *CA Cancer J Clin*. 2024;74(3):229–263. doi:10.3322/caac.21834
3. Kim DY. Changing etiology and epidemiology of hepatocellular carcinoma: Asia and worldwide. *J Liver Cancer*. 2024;24(1):62–70. doi:10.17998/jlc.2024.03.13
4. Lampimukhi M, Qassim T, Venu R, et al. A Review of Incidence and Related Risk Factors in the Development of Hepatocellular Carcinoma. *Cureus*. 2023;15(11):e49429. doi:10.7759/cureus.49429
5. Chen Y, Wang W, Morgan MP, Robson T, Annett S. Obesity, non-alcoholic fatty liver disease and hepatocellular carcinoma: current status and therapeutic targets. *Front Endocrinol*. 2023;14:1148934. doi:10.3389/fendo.2023.1148934
6. Li C, Lu B, Deng B. New Insights into the Diagnosis and Treatment of Hepatocellular Carcinoma. *Biomedicines*. 2025;13(5):1244. doi:10.3390/biomedicines13051244
7. Patauner S, Scotton G, Notte F, Frena A. Advanced hepatocellular carcinoma treatment strategies: are transarterial approaches leading the way? *World J Gastrointest Oncol*. 2025;17(1):99834. doi:10.4251/wjgo.v17.i1.99834
8. Liu Q, Zhang R, Shen W. Advancements in locoregional therapy for advanced hepatocellular carcinoma: emerging perspectives on combined treatment strategies. *Eur J Surg Oncol*. 2025;51(2):109502. doi:10.1016/j.ejso.2024.109502
9. Gujarathi R, Franses JW, Pillai A, Liao CY. Targeted therapies in hepatocellular carcinoma: past, present, and future. *Front Oncol*. 2024;14:1432423. doi:10.3389/fonc.2024.1432423
10. Bloom M, Podder S, Dang H, Lin D. Advances in Immunotherapy in Hepatocellular Carcinoma. *Int J Mol Sci*. 2025;26(5):1936. doi:10.3390/ijms26051936

11. Kunji ERS, King MS, Ruprecht JJ, Thangaratnarajah C. The SLC25 Carrier Family: important Transport Proteins in Mitochondrial Physiology and Pathology. *Physiology*. 2020;35(5):302–327. doi:10.1152/physiol.00009.2020
12. Gao R, Zhou D, Qiu X, et al. Cancer Therapeutic Potential and Prognostic Value of the SLC25 Mitochondrial Carrier Family: a Review. *Cancer Control*. 2024;31:10732748241287905. doi:10.1177/10732748241287905
13. Yu HC, Bai L, Jin L, Zhang YJ, Xi ZH, Wang DS. SLC25A35 enhances fatty acid oxidation and mitochondrial biogenesis to promote the carcinogenesis and progression of hepatocellular carcinoma by upregulating PGC-1α. *Cell Commun Signal*. 2025;23(1):130. doi:10.1186/s12964-025-02109-y
14. Zhang Q, Wei T, Jin W, et al. Deficiency in SLC25A15, a hypoxia-responsive gene, promotes hepatocellular carcinoma by reprogramming glutamine metabolism. *J Hepatol*. 2024;80(2):293–308. doi:10.1016/j.jhep.2023.10.024
15. Yuan P, Mu J, Wang Z, et al. Down-regulation of SLC25A20 promotes hepatocellular carcinoma growth and metastasis through suppression of fatty-acid oxidation. *Cell Death Dis*. 2021;12(4):361. doi:10.1038/s41419-021-03648-1
16. Ding YH, Huang TY, Xu SM, et al. Inhibition of SLC25A10 promotes cellular senescence and impedes hepatocellular carcinoma progression. *Transl Cancer Res*. 2025;14(8):4939–4954. doi:10.21037/tcr-2024-2319
17. Seifert EL, Ligeti E, Mayr JA, Sondheimer N, Hajnoczky G. The mitochondrial phosphate carrier: role in oxidative metabolism, calcium handling and mitochondrial disease. *Biochem Biophys Res Commun*. 2015;464(2):369–375. doi:10.1016/j.bbrc.2015.06.031
18. Zabit S, Melloul O, Lichtenstein M, Seifert EL, Lorberboum-Galski H. Rescue of the First Mitochondrial Membrane Carrier, the mPiC, by TAT-Mediated Protein Replacement Treatment. *Int J Mol Sci*. 2025;26(9):4379. doi:10.3390/ijms26094379
19. Boulet A, Vest KE, Maynard MK, et al. The mammalian phosphate carrier SLC25A3 is a mitochondrial copper transporter required for cytochrome c oxidase biogenesis. *J Biol Chem*. 2018;293(6):1887–1896. doi:10.1074/jbc.RA117.000265
20. Wang JH, Wu XJ, Duan YZ, Li F. Circular RNA_CNST Promotes the Tumorigenesis of Osteosarcoma Cells by Sponging miR-421. *Cell Transplant*. 2020;29:963689720926147. doi:10.1177/0963689720926147
21. Nakanishi T, Kawasaki Y, Nakamura Y, et al. An implication of the mitochondrial carrier SLC25A3 as an oxidative stress modulator in NAFLD. *Exp Cell Res*. 2023;431(1):113740. doi:10.1016/j.yexcr.2023.113740
22. Hanzelmann S, Castelo R, Guinney J. GSVA: gene set variation analysis for microarray and RNA-seq data. *BMC Bioinf*. 2013;14:7. doi:10.1186/1471-2105-14-7
23. Liu CJ, Hu FF, Xie GY, et al. GSCA: an integrated platform for gene set cancer analysis at genomic, pharmacogenomic and immunogenomic levels. *Brief Bioinform*. 2023;24(1):bbac558. doi:10.1093/bib/bbac558
24. Liu S, Zhang P, Wu Y, et al. SLC25A19 is a novel prognostic biomarker related to immune invasion and ferroptosis in HCC. *Int Immunopharmacol*. 2024;136:112367. doi:10.1016/j.intimp.2024.112367
25. Zhang Z, Qiao Y, Sun Q, Peng L, Sun L. A novel SLC25A1 inhibitor, parthenolide, suppresses the growth and stemness of liver cancer stem cells with metabolic vulnerability. *Cell Death Discov*. 2023;9(1):350. doi:10.1038/s41420-023-01640-6
26. Chen L, Ying X, Xie J, Liu H, Liu W. SLC25A19 is a key prognostic marker for hepatocellular carcinoma. *Sci Rep*. 2025;15(1):13435. doi:10.1038/s41598-025-98371-8
27. Sheng M, Zhang Y, Wang Y, et al. Decoding the role of aberrant RNA alternative splicing in hepatocellular carcinoma: a comprehensive review. *J Cancer Res Clin Oncol*. 2023;149(19):17691–17708. doi:10.1007/s00432-023-05474-8
28. Lv X, Sun X, Gao Y, et al. Targeting RNA splicing modulation: new perspectives for anticancer strategy? *J Exp Clin Cancer Res*. 2025;44(1):32. doi:10.1186/s13046-025-03279-w
29. Wang X, Liu W, Zhan C, et al. Alternative splicing of EZH2 regulated by SNRPB mediates hepatocellular carcinoma progression via BMP2 signaling pathway. *iScience*. 2025;28(1):111626. doi:10.1016/j.isci.2024.111626



**Journal of Hepatocellular Carcinoma**

**Dovepress**
Taylor & Francis Group

**Publish your work in this journal**

The Journal of Hepatocellular Carcinoma is an international, peer-reviewed, open access journal that offers a platform for the dissemination and study of clinical, translational and basic research findings in this rapidly developing field. Development in areas including, but not limited to, epidemiology, vaccination, hepatitis therapy, pathology and molecular tumor classification and prognostication are all considered for publication. The manuscript management system is completely online and includes a very quick and fair peer-review system, which is all easy to use. Visit http://www.dovepress.com/testimonials.php to read real quotes from published authors.

**Submit your manuscript here:** https://www.dovepress.com/journal-of-hepatocellular-carcinoma-journal